Searches for Higgs pair production at LHC

Kun Liu (TDLI/SJTU)

The 6th China LHC Physics workshop

@Tsinghua Uni. (Virtual), 2020.11.07

Outline

I. Introduction

II. Run 2 results from ATLAS and CMS experiments

III. Prospects at HL-LHC

IV. Summary

Why do we care about Higgs pair production

- ✦ Higgs precision measurements are in good agreement with the SM predictions by far.
- ✦ Higgs pair production is rare in the SM (31.05fb@NNLO)
  - ✦ It has not been observed yet
  - ✦ It allows direct access to the Higgs self-coupling
- ✦ Many BSM models enhance di-Higgs production rate, e.g 2HDMs, hMSSM, EWK-singlet …
- ✦ LHC + HL-LHC is unique factory for di-Higgs searches
  - ✦ energy frontier ($\sqrt{s}$ = 7/8/13/14 TeV)
  - ✦ good integrated luminosity (300/3000fb^{-1})

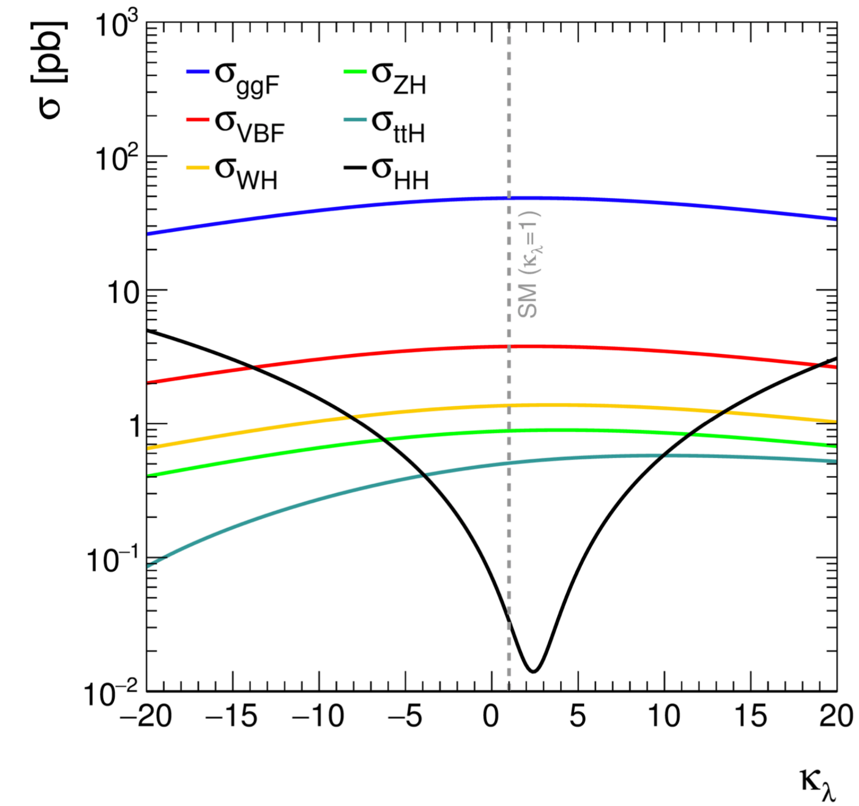

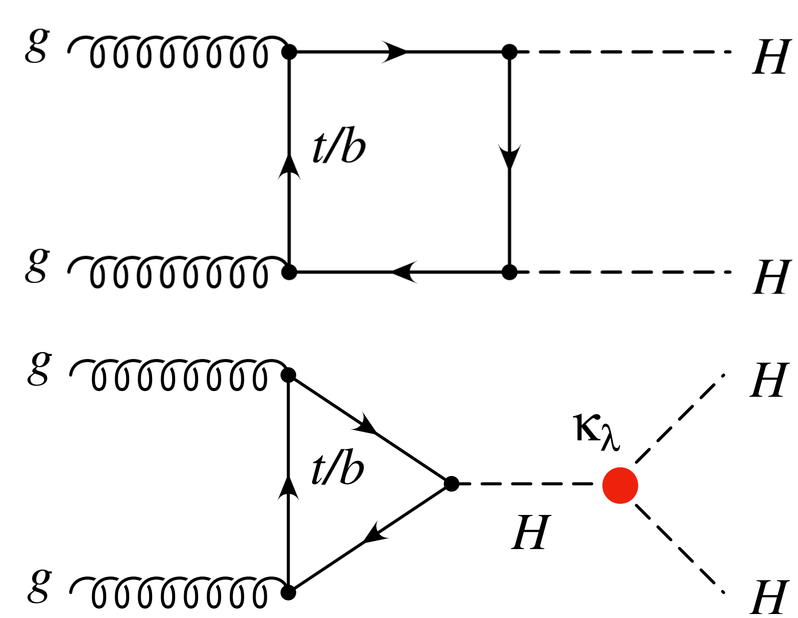

Analysis data luminosity

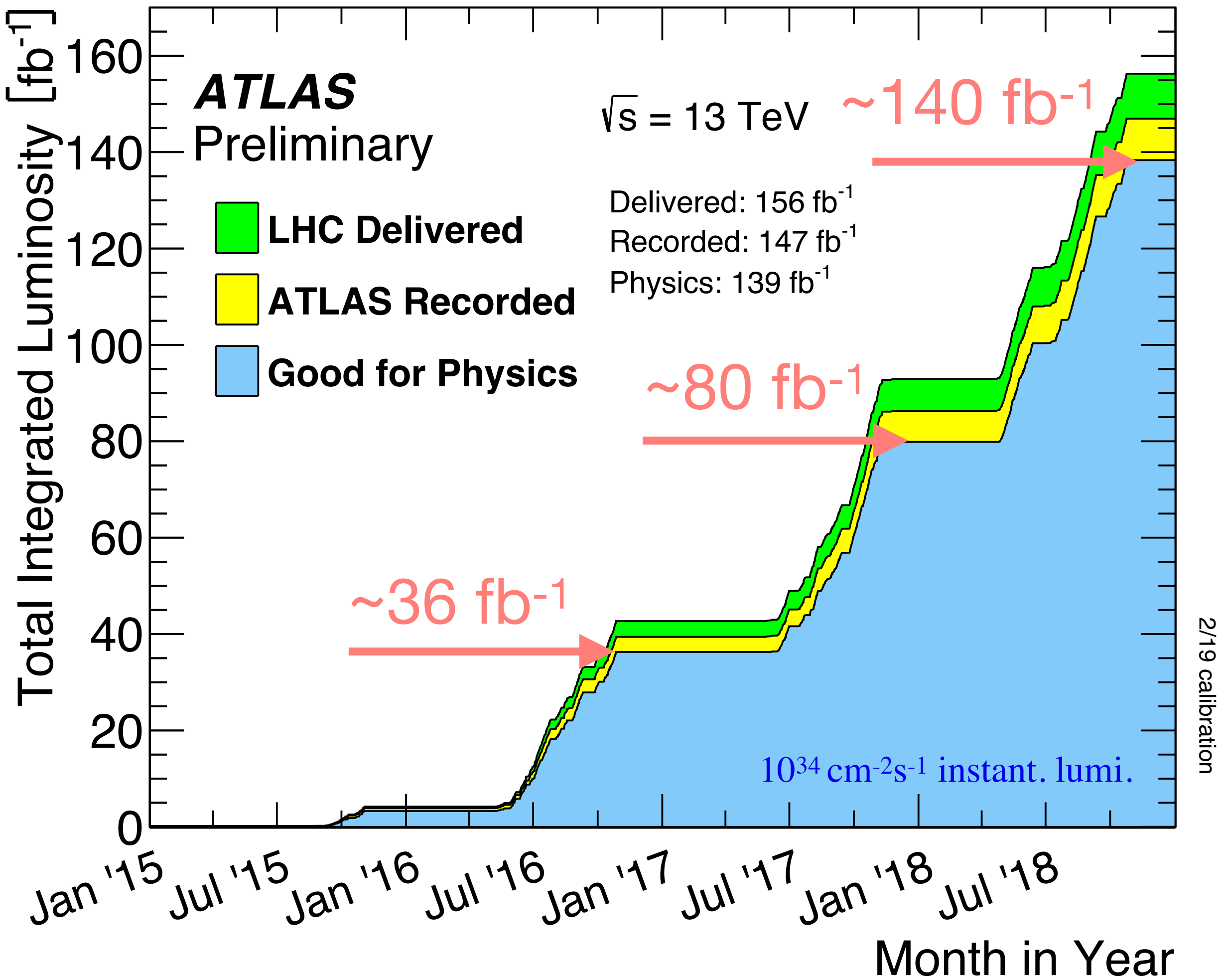

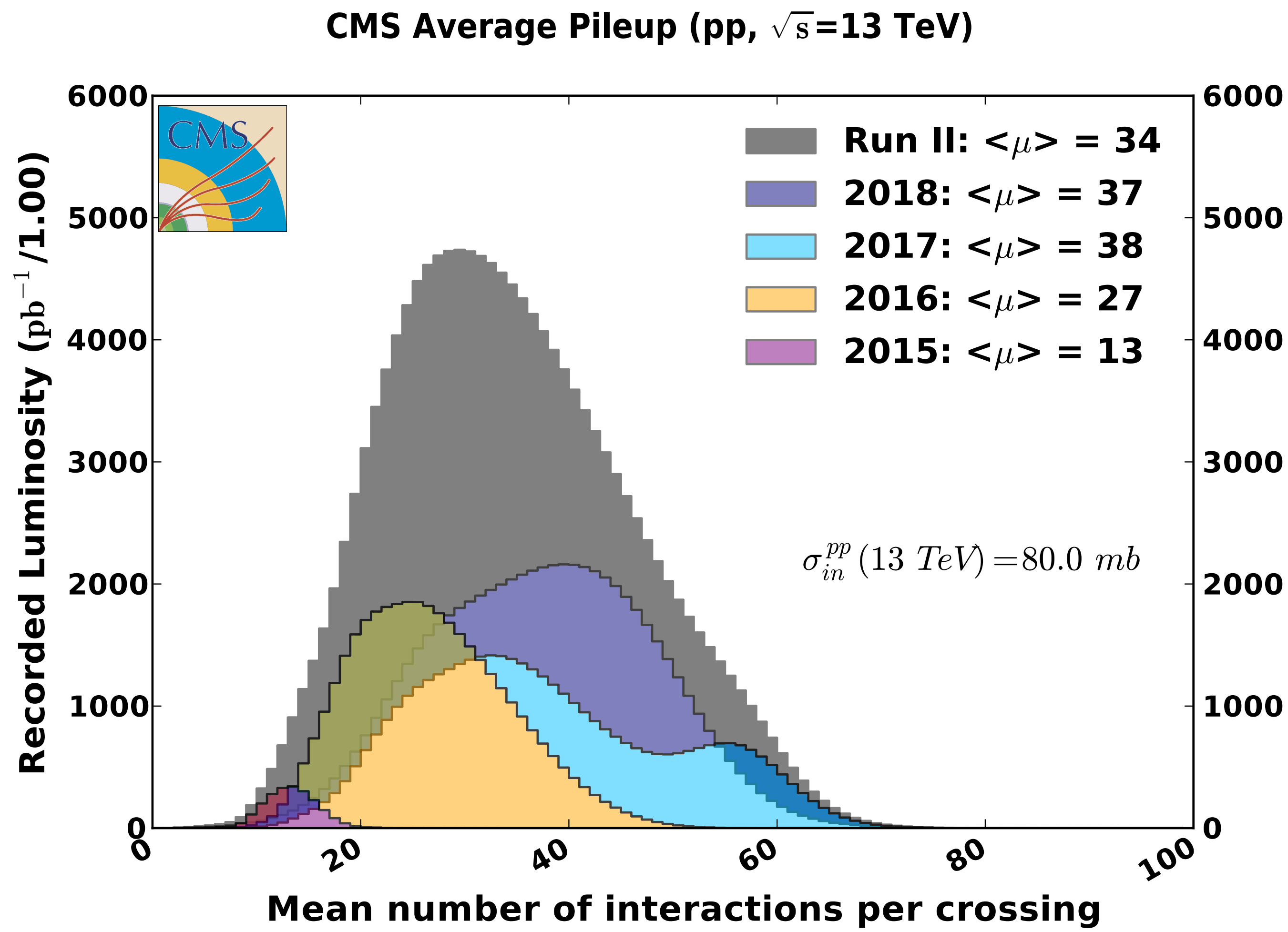

- ATLAS and CMS experiments have successfully collected ~140 fb^{-1} luminosity at 13 TeV centre-of-mass energy in full Run 2 period → Thanks to LHC machine !
- Run 2 dataset has been used in stages for published analyses: 36 / 80 / 140 fb^{-1}.
- Each experiment has produced ~4300 HH events in SM expectation (σ_{HH}=31.05fb@NNLO).

Higgs pair decay signatures

Di-Higgs decay branching ratios

rarer →

↓ rarer

	bb	WW	gg	ττ	cc	ZZ	γγ	Zγ	μμ
bb	33%								
WW	25%	4.6%							
gg									
ττ	7.4%								
cc									
ZZ	3.1%								
γγ	0.26%	0.1%							
Zγ									
μμ									

HH→4b

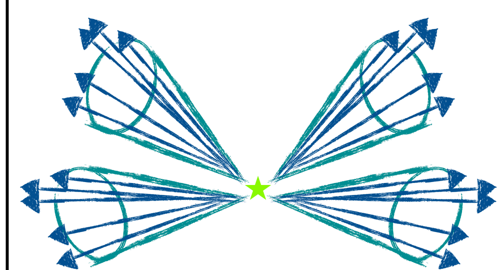

Picture from E. Brost

- The highest branching ratio
- Large QCD multi-jet background.

HH→bbττ

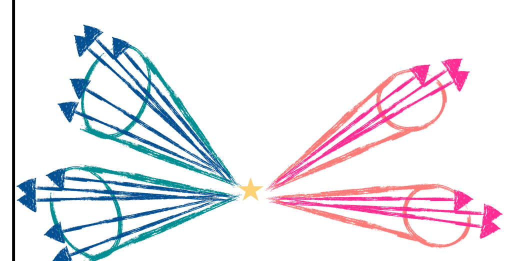

Picture from E. Brost

- Relatively large branching ratio
- Cleaner final state.

There are also **bbWW, bbZZ, 4W** channels

- relatively large branching ratios
- final states can be reconstructed

and **WWγγ** channel having clean signal.

HH→bbγγ

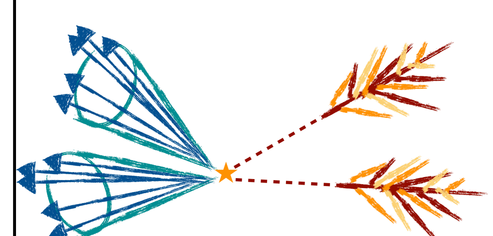

Picture from E. Brost

- Small branching ratio
- Clean final state
- Narrow H→γγ peak on top of continuum bkg.

Event reconstruction and discriminating variables

Non-resonant HH

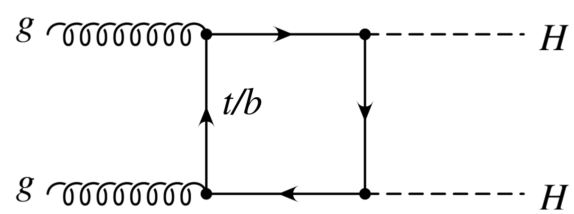

Higgs candidate can be reconstructed

- from $\gamma\gamma$ (good resolution)
- from bb, $\tau\tau$

Resonant HH

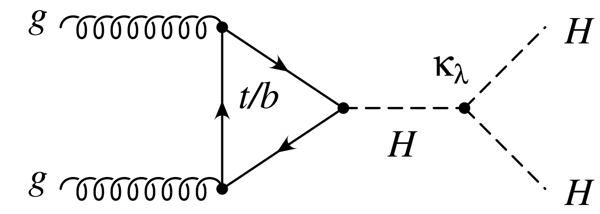

Di-Higgs candidate reconstruction from 4-body invariant mass m_{HH}.

m_{HH} is also used for resonance searches.

Multi-variate discriminators are used to incorporate many variables.

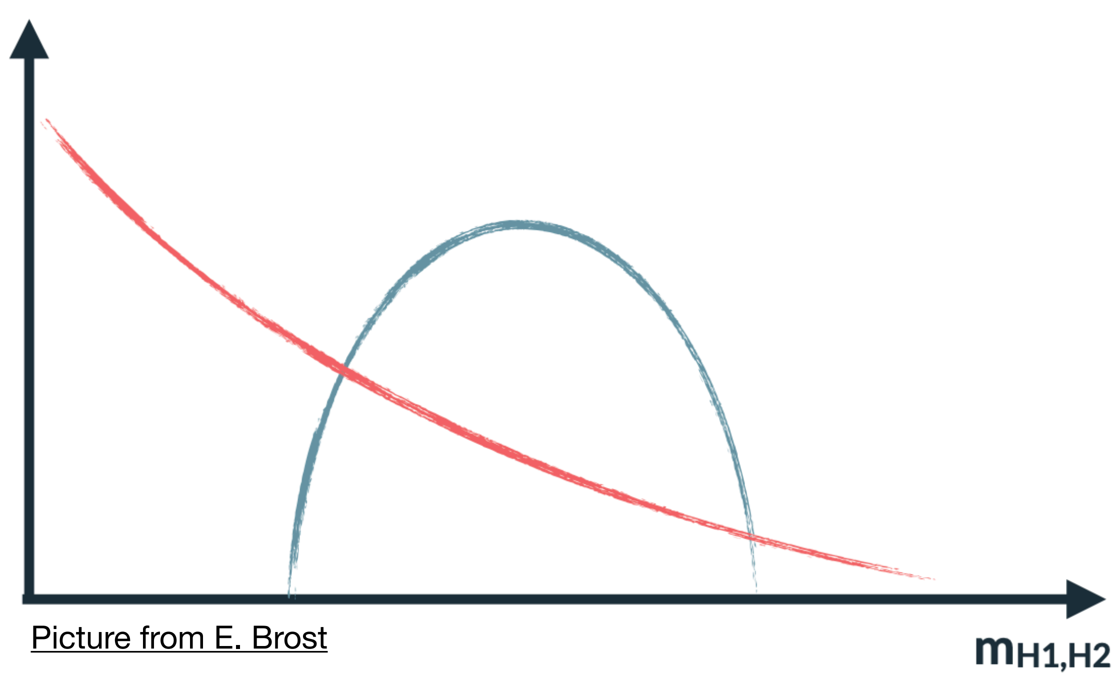

Picture from E. Brost

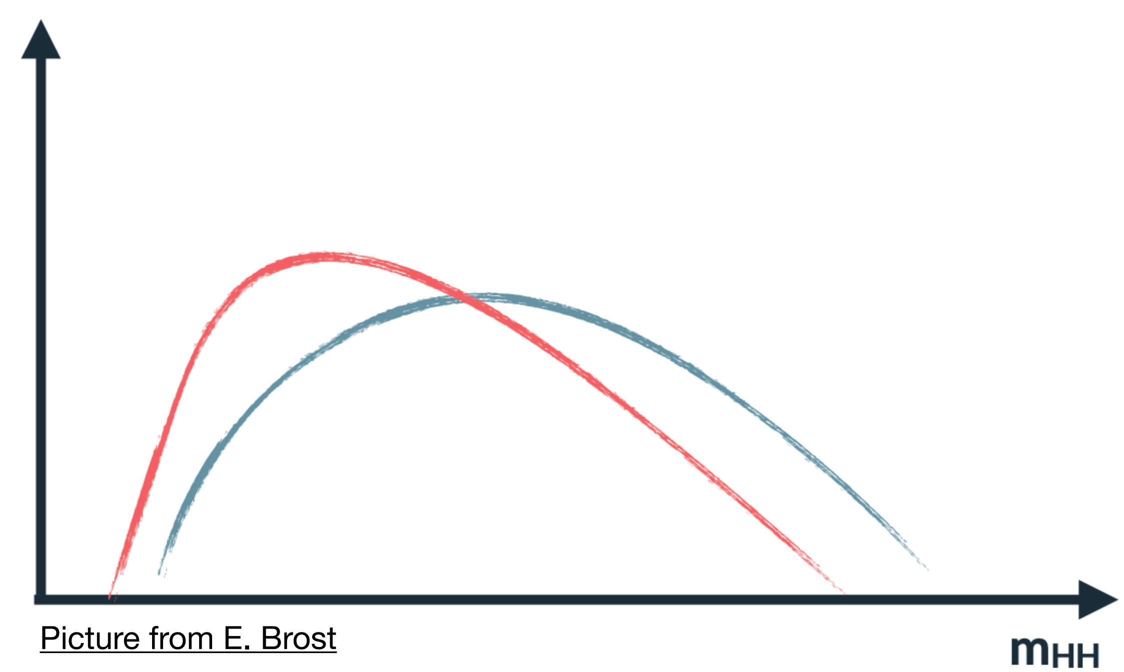

Picture from E. Brost

Discrimination distributions (m_{H1},m_{H2}; m_{HH}) for signal and background processes.

Event reconstruction and discriminating variables

Non-resonant HH

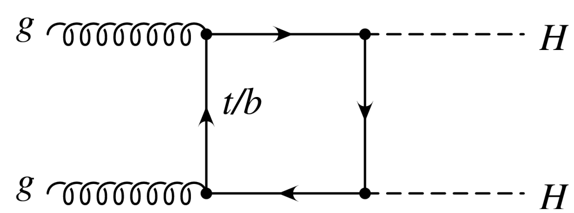

Higgs candidate can be reconstructed

- from $\gamma\gamma$ (good resolution)
- from bb, $\tau\tau$

Resonant HH

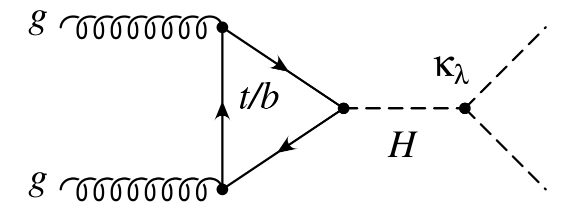

Di-Higgs candidate reconstruction from 4-body invariant mass m_{HH}.

m_{HH} is also used for resonance searches

Multi-variate discriminators are used to incorporate many variables.

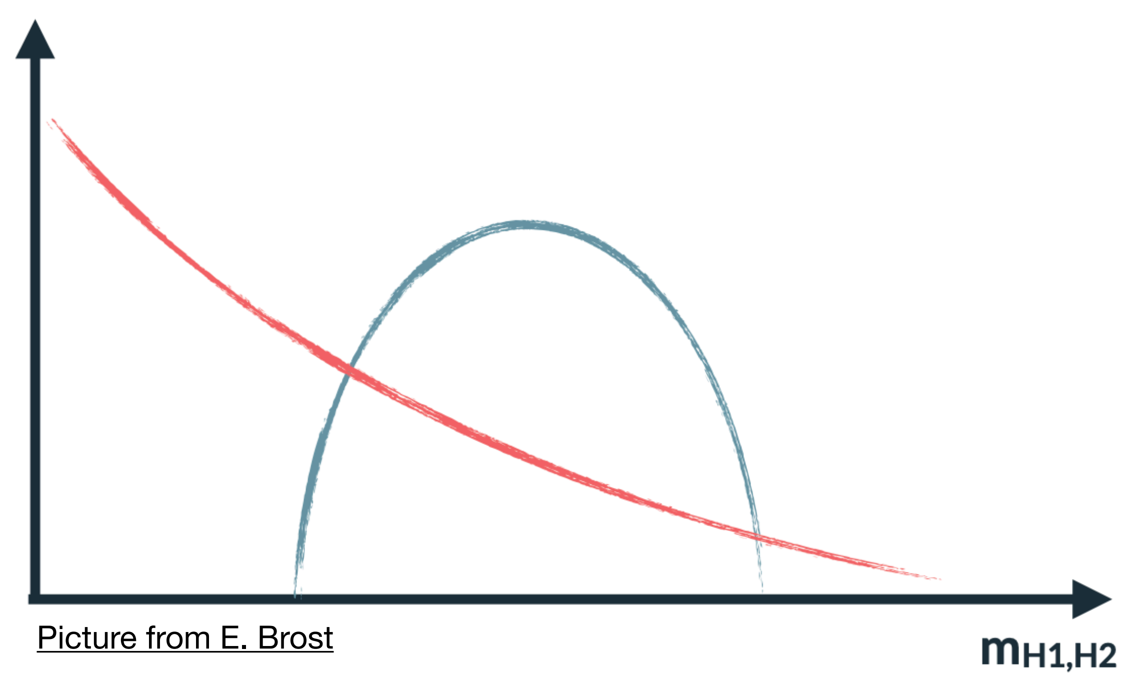

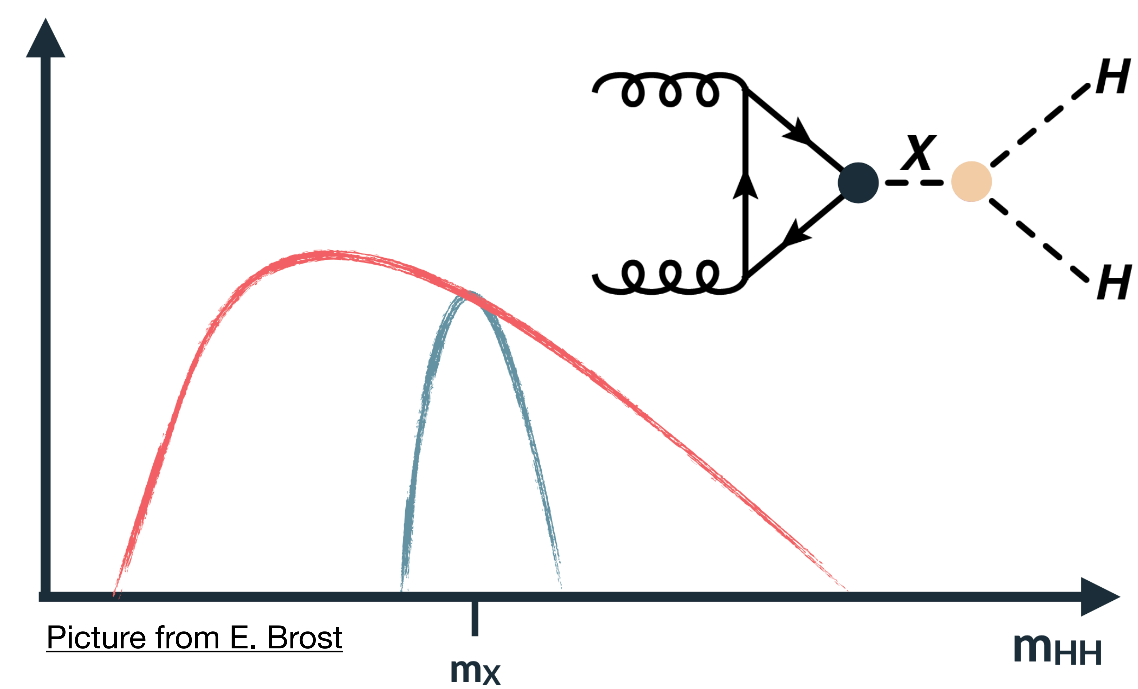

Discrimination distributions (m_{H1},m_{H2}; m_{HH}) for signal and background processes.

Event reconstruction and discriminating variables

- Non-resonant and resonant HH contributions to the m_{HH} spectrum.

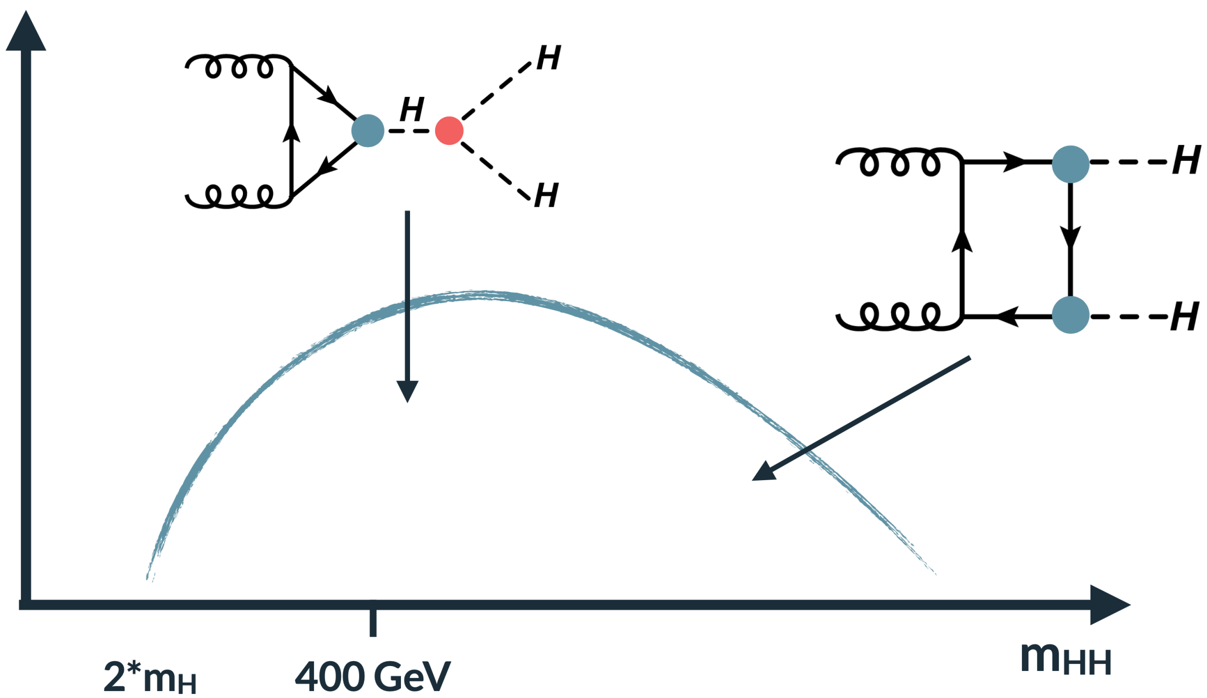

Picture from E. Brost

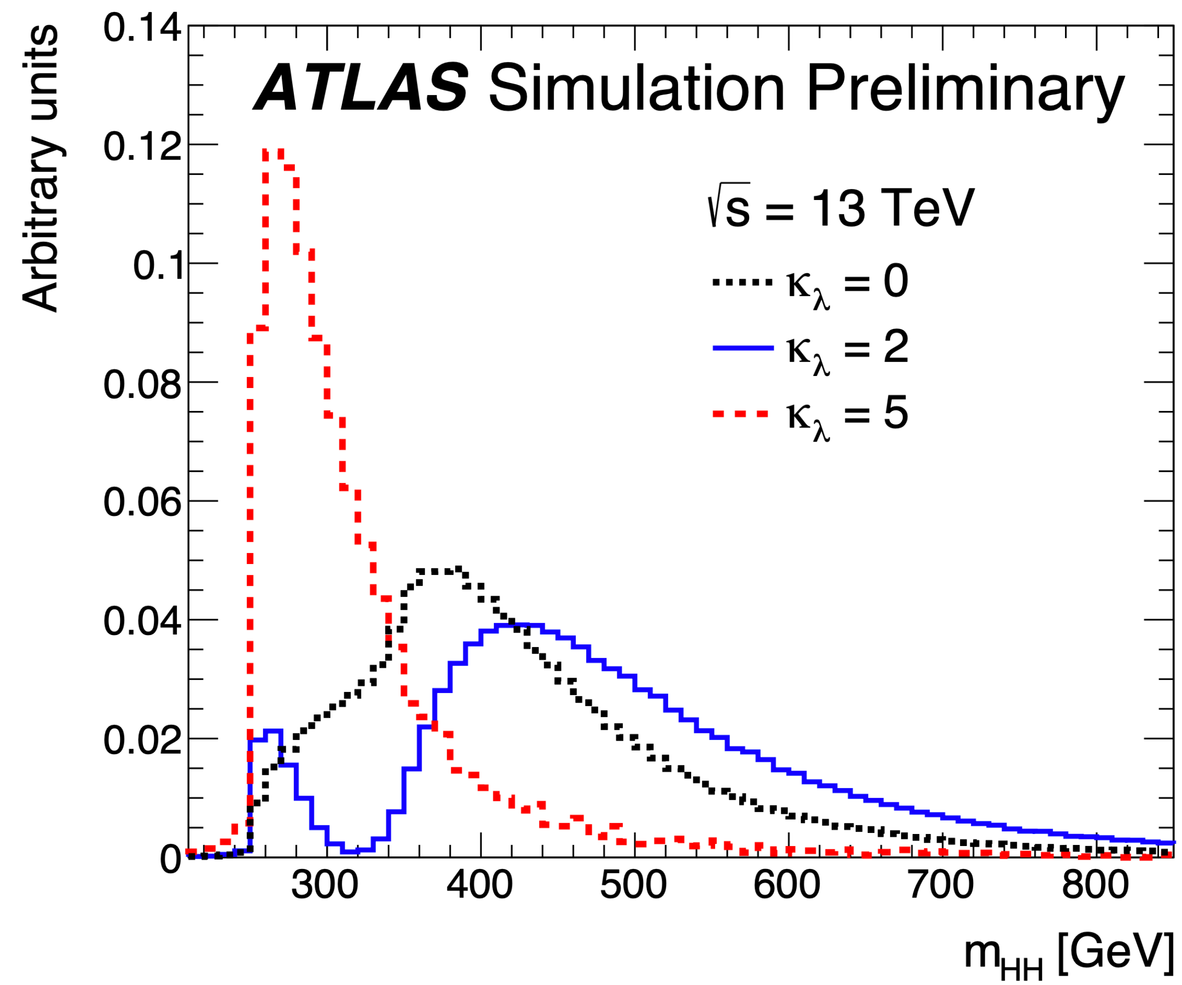

- Non-resonant HH process contributes more at m_{HH} harder regions
  - $\kappa_\lambda = 0$, contribution only from box diagrams
  - $\kappa_\lambda \geq 5$, resonant process dominates
  - $\kappa_\lambda = 2$, maximal destructive interference

ATLAS and CMS analysis channel and status

Channel	ATLAS	CMS
4b	JHEP 01 (2019) 030 36.1 fb^{-1} JHEP 07 (2020) 108 (VBF) 127 fb^{-1}	JHEP04(2019)112 35.9fb^{-1}
$bb\tau\tau$	Phys. Rev. Lett. 121 (2018) 191801 36.1 fb^{-1} Acc. by JHEP (boosted) 139 fb^{-1}	Phys.Lett.B 778 (2018) 101-127 35.9 fb^{-1}
$bb\gamma\gamma$	JHEP 11 (2018) 040 36.1 fb^{-1}	CMS-PAS-HIG-19-018 137 fb^{-1}
bbWW	JHEP 04 (2019) 092 (lvqq) 36.1 fb^{-1} Phys. Lett. B 801(2020)135145 (lvlv) 139 fb^{-1}	JHEP01(2018)054 35.9 fb^{-1}
4W	JHEP 05 (2019) 124 36.1 fb^{-1}	/
$WW\gamma\gamma$	Eur. Phys. J. C 78 (2018) 1007 36.1 fb^{-1}	/
bbZZ	/	CMS-PAS-HIG-20-004 137 fb^{-1}
Combination	Phys. Lett. B 800 (2020) 135103 36.1 fb^{-1}	Phys.Rev.Lett. 122(2019)121803 35.9 fb^{-1}

* green color marks for those analyses being updated with full run 2 luminosity.

Limits on Higgs pair production cross section

- 95%C.L. upper limit on σ_{HH} is 6.9 and 7.7 from ATLAS and CMS experiment.
- Dominant channels: HH→bb$\tau\tau$, 4b and bb$\gamma\gamma$.

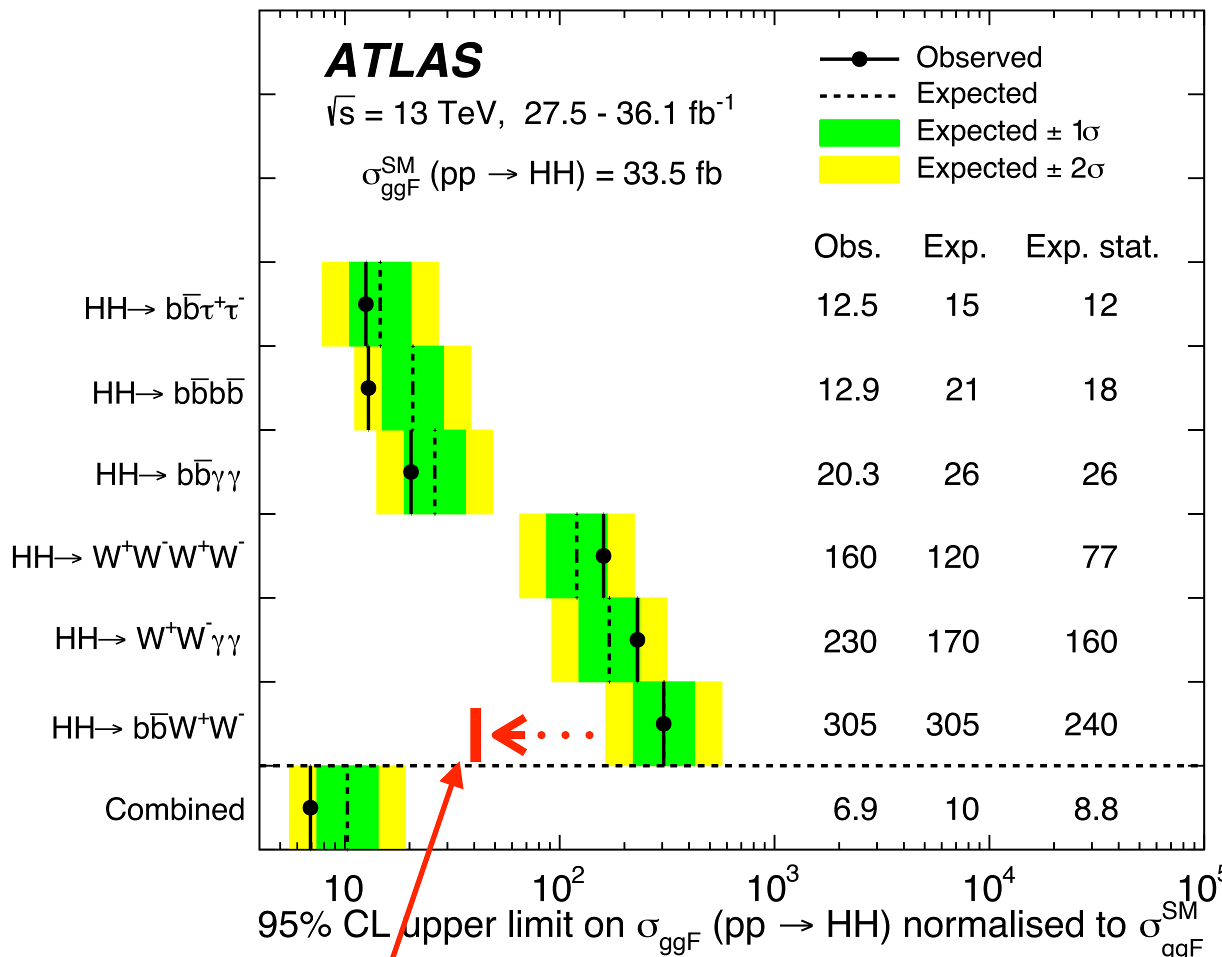

New bbWW obs (exp.) limit: 40 (29^{+14}_{-9}) with full Run 2 luminosity (139fb^{-1})

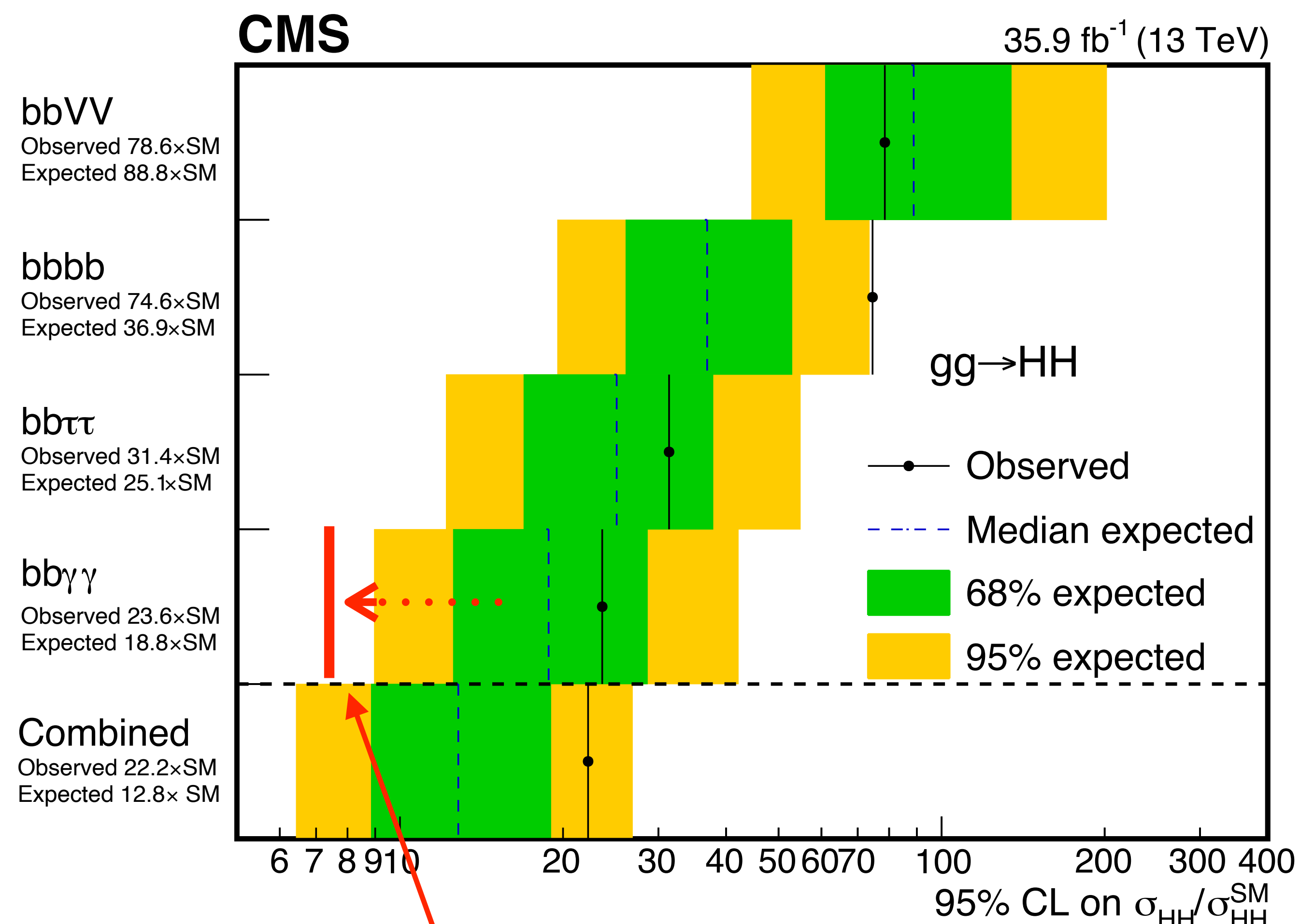

New bb$\gamma\gamma$ obs.(exp.) limit: 7.7 (5.2) with full Run 2 luminosity (137fb^{-1})

Limits on Higgs self-coupling

- κ_λ is limited to [-5.0, 12.0] and [-3.3, 8.5] from ATLAS and CMS experiment.
- CMS HH→bb$\gamma\gamma$ channel has used full Run 2 luminosity (137fb^{-1}).

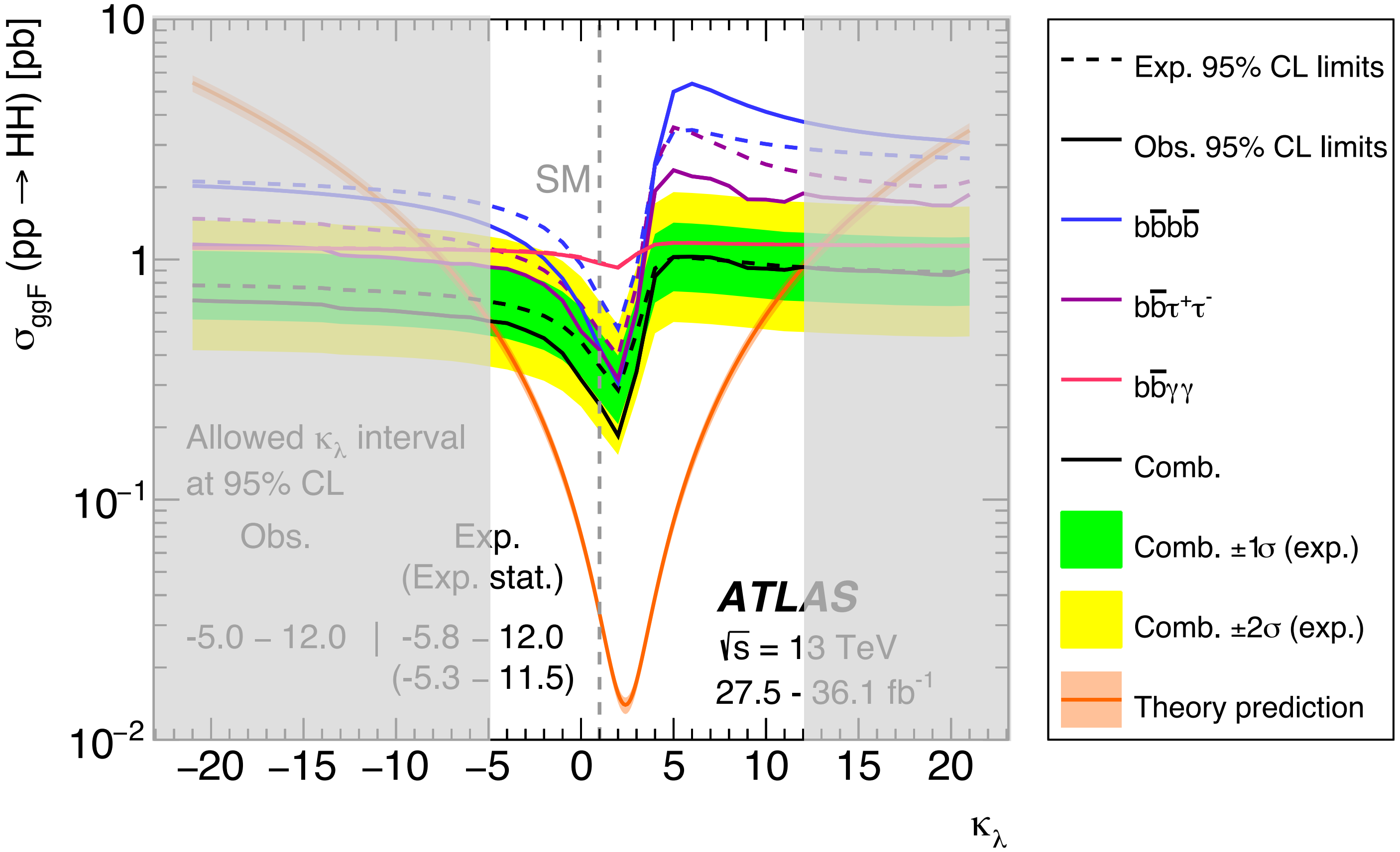

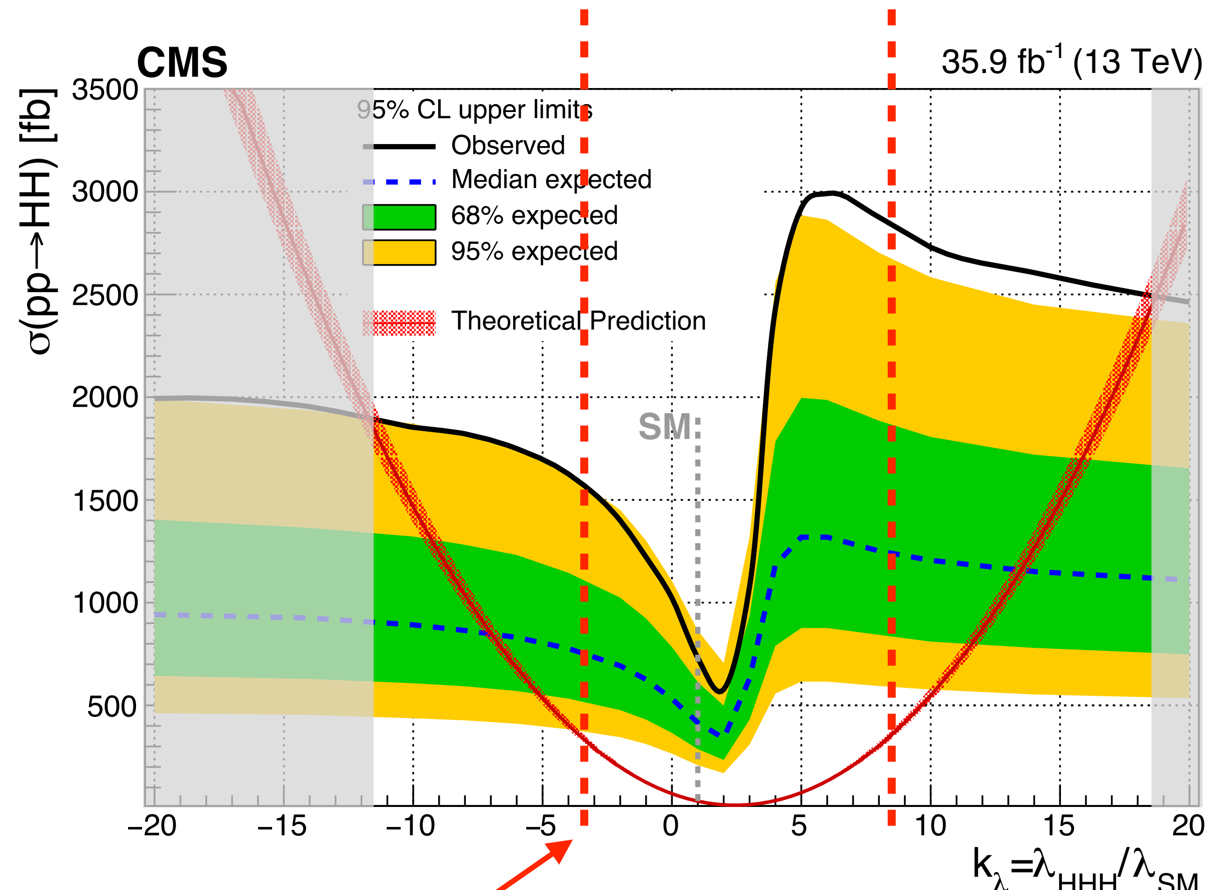

New bb$\gamma\gamma$ result: [-3.3, 8.5] with full Run 2 luminosity (137fb^{-1})

Limits on narrow resonance production cross section

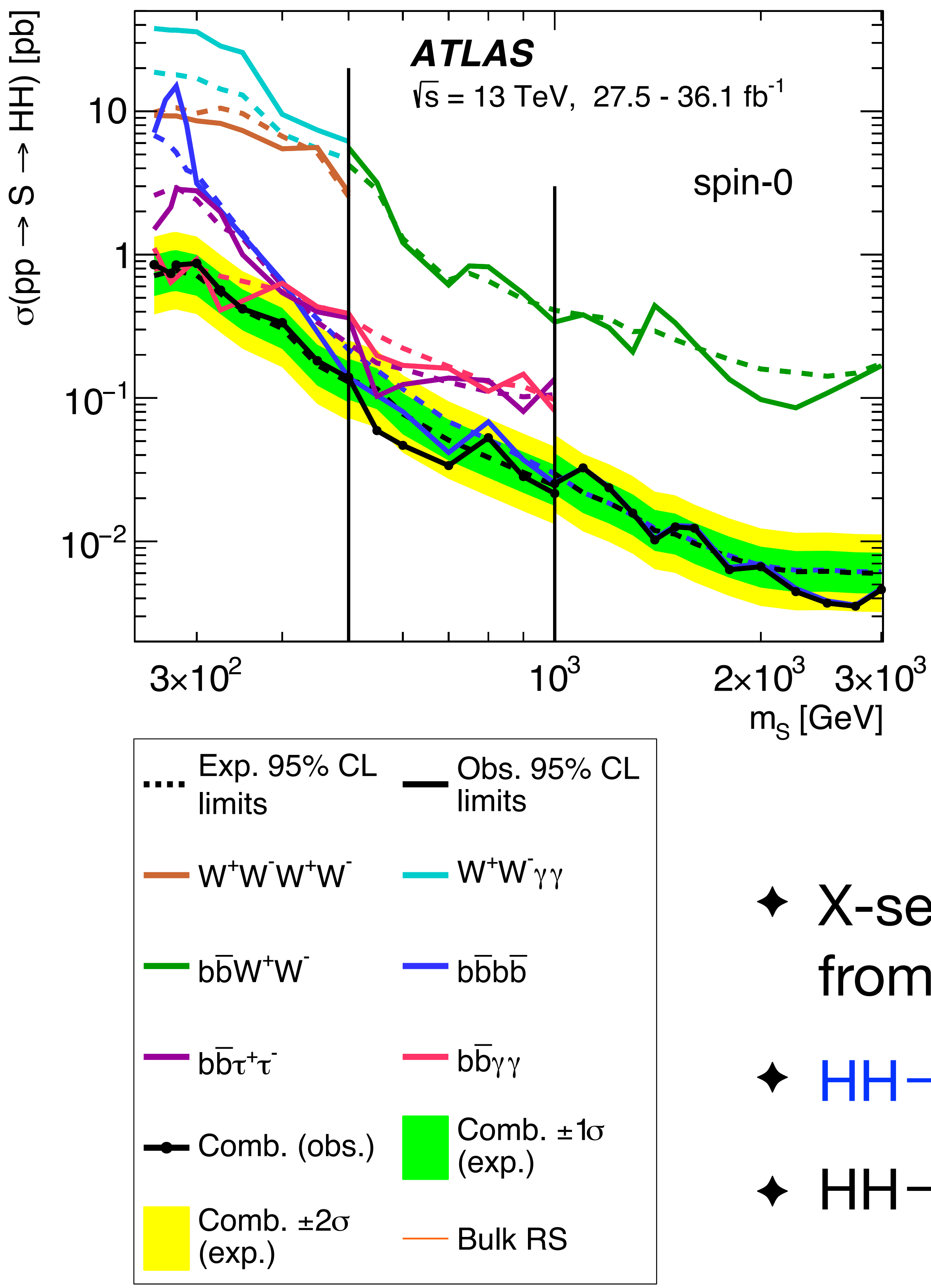

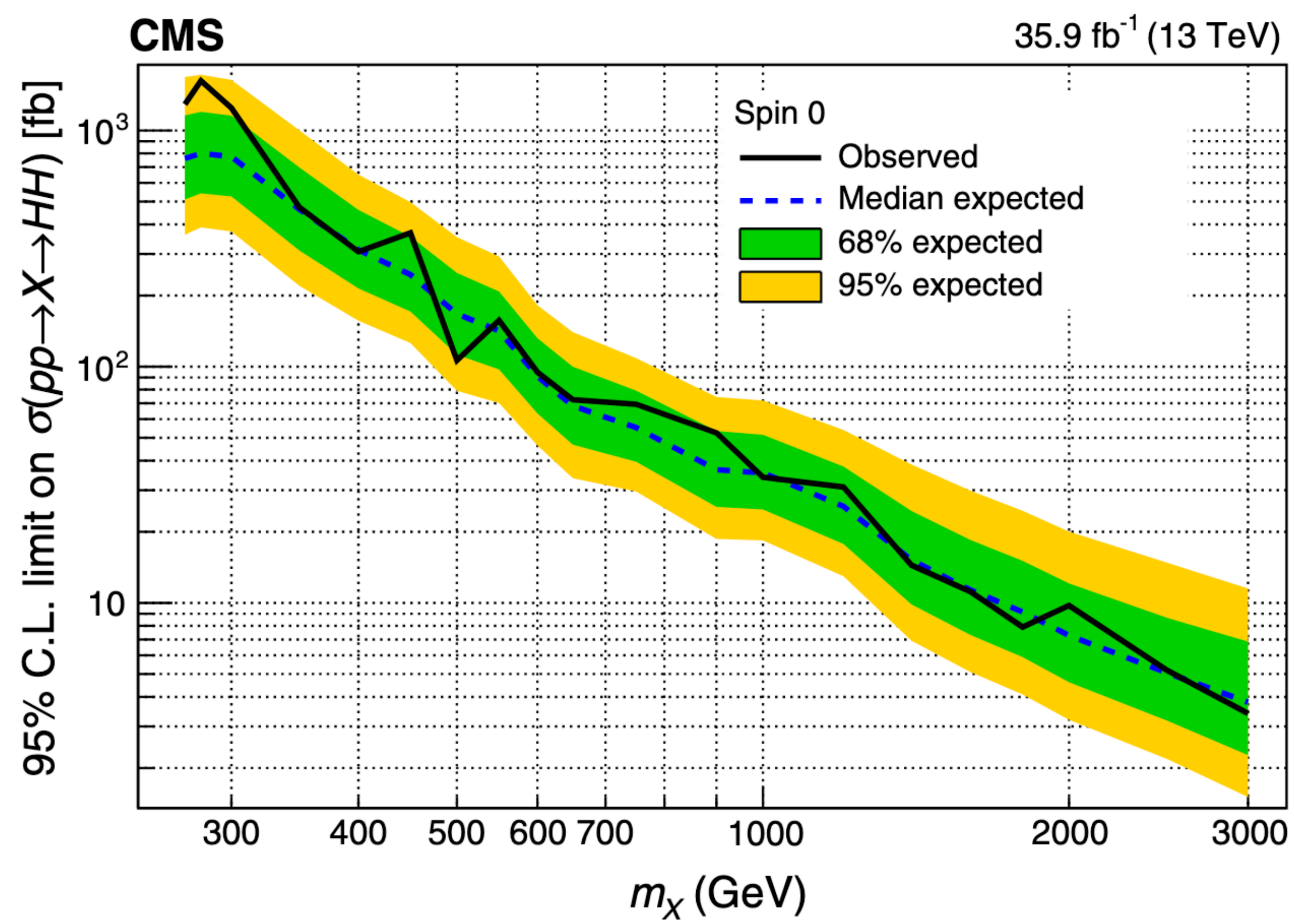

- X-section limit for narrow resonant particle varies from ~1pb to ~3fb in [260GeV, 3TeV] mass range.
- HH→4b dominates > 600GeV mass regime.
- HH→bbγγ dominates [260,400] GeV mass regime.

VBF HH searches in 4b and bbγγ channels

- VBF HH has unique sensitivity to VVHH coupling (κ_{2V}).
- Regions out of which have been excluded at 95%C.L.
  - from ATLAS HH→4b (126fb^{-1}): [-0.76, 2.90]
  - from CMS HH→bbγγ (137fb^{-1}): [-1.3, 3.5]

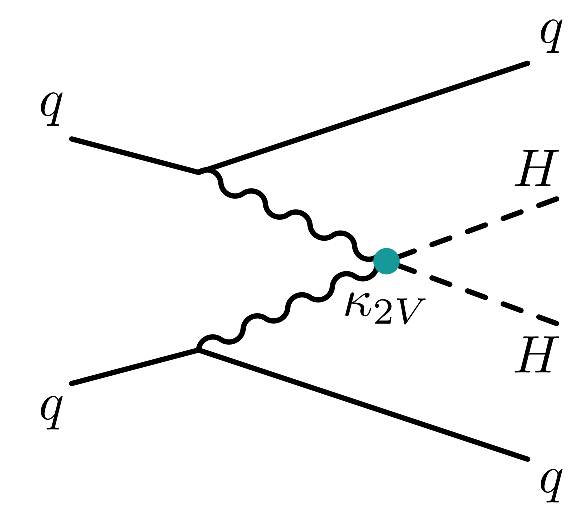

ATLAS HH→4b channel

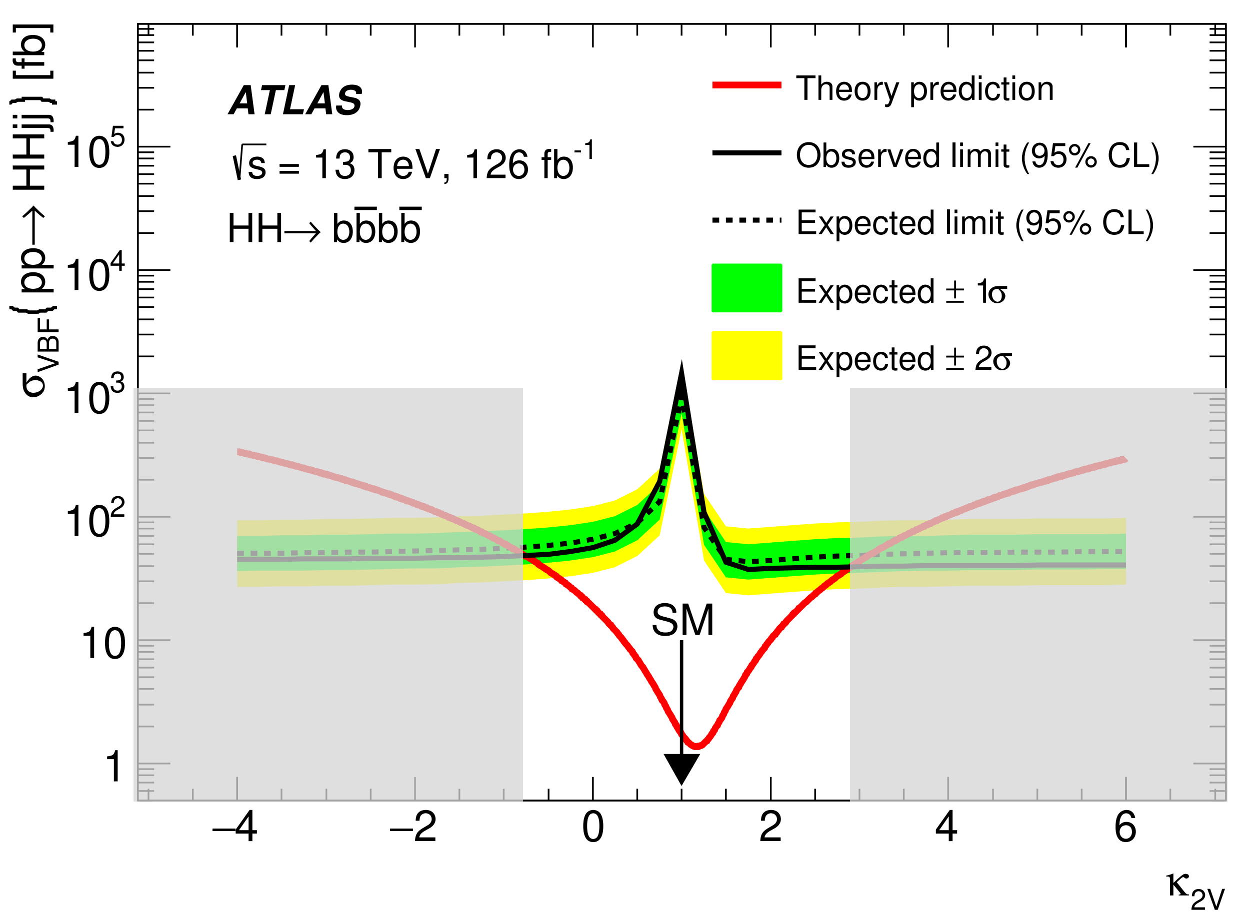

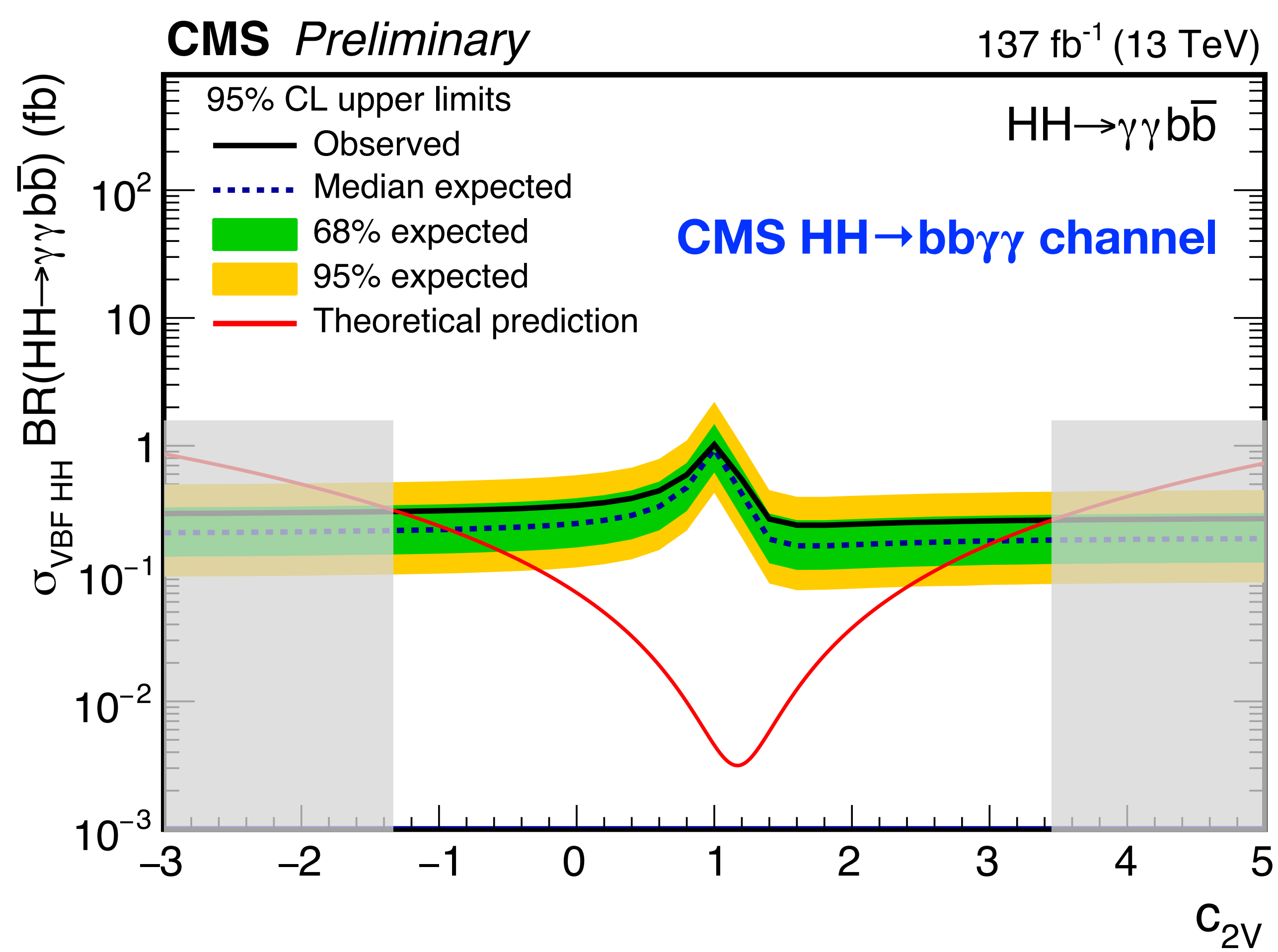

First bbZZ(→4l) result from CMS (137 fb^{-1})

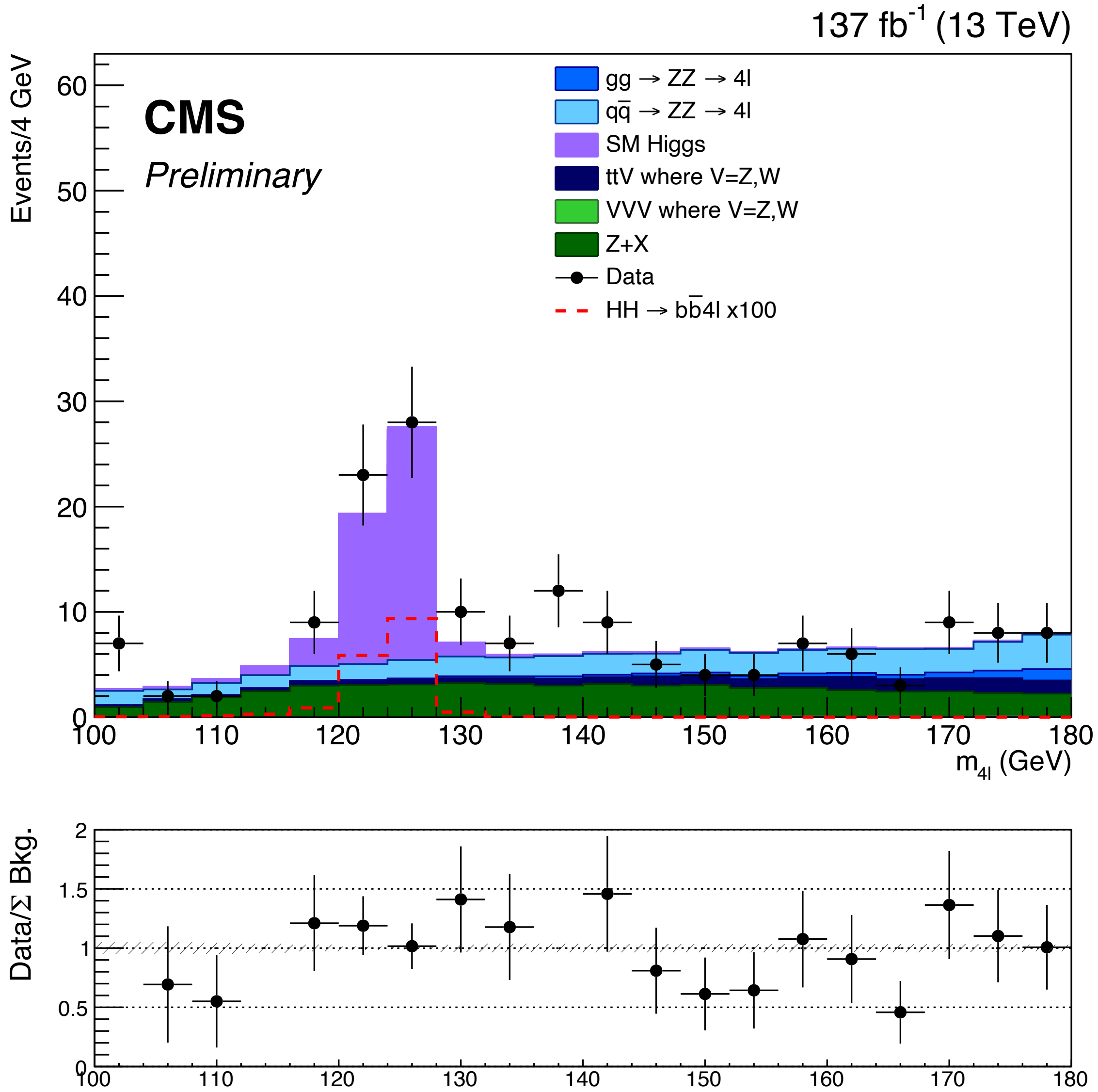

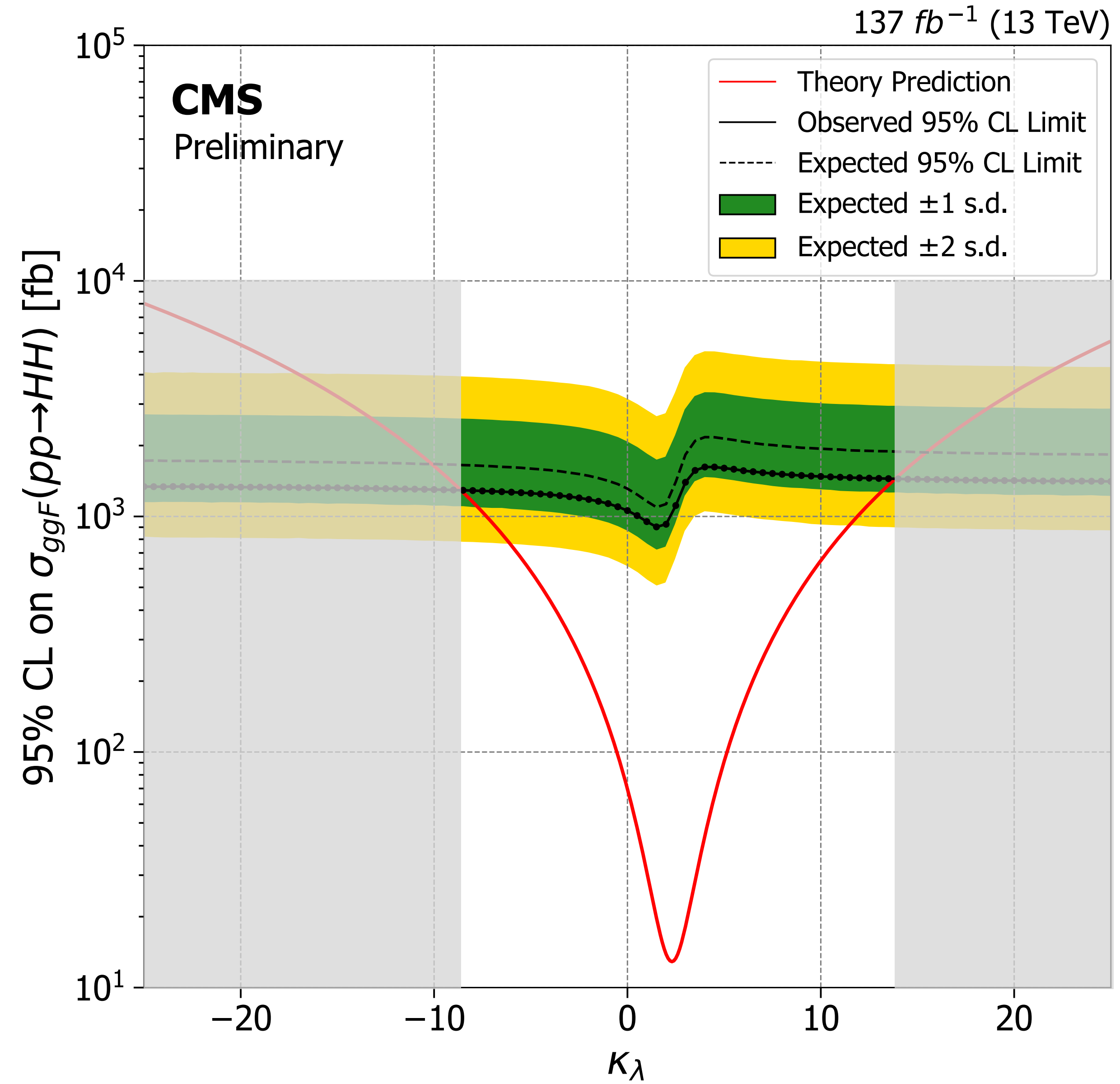

- First HH→bbZZ(→4l) search has been performed in CMS (137 fb^{-1})
  - Obs. (exp.) limit on X-section is 30(37) times the SM prediction
  - Limit on self-coupling parameter κ_λ: [-9, 14].

Boosted HH→bb$\tau\tau$ search in ATLAS (139fb^{-1})

- Reconstruction and identification of boosted di-tau systems, using large-radius jets and exploiting jet substructure.
- Obs. limits on X→HH production cross-section lie between 94pb and 28pb for X mass in the range 1.0 - 3.0 TeV.

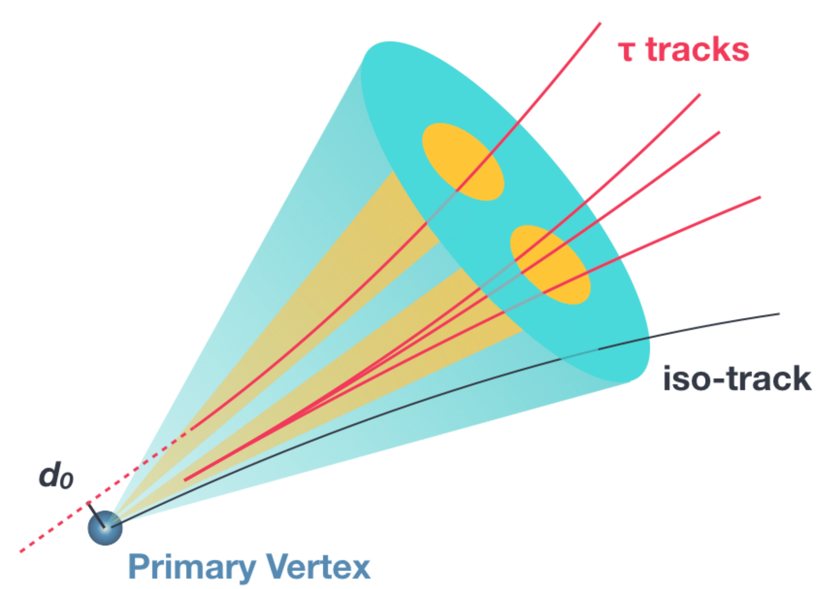

Identify two tau candidates as "subjects" in a large-R jet.

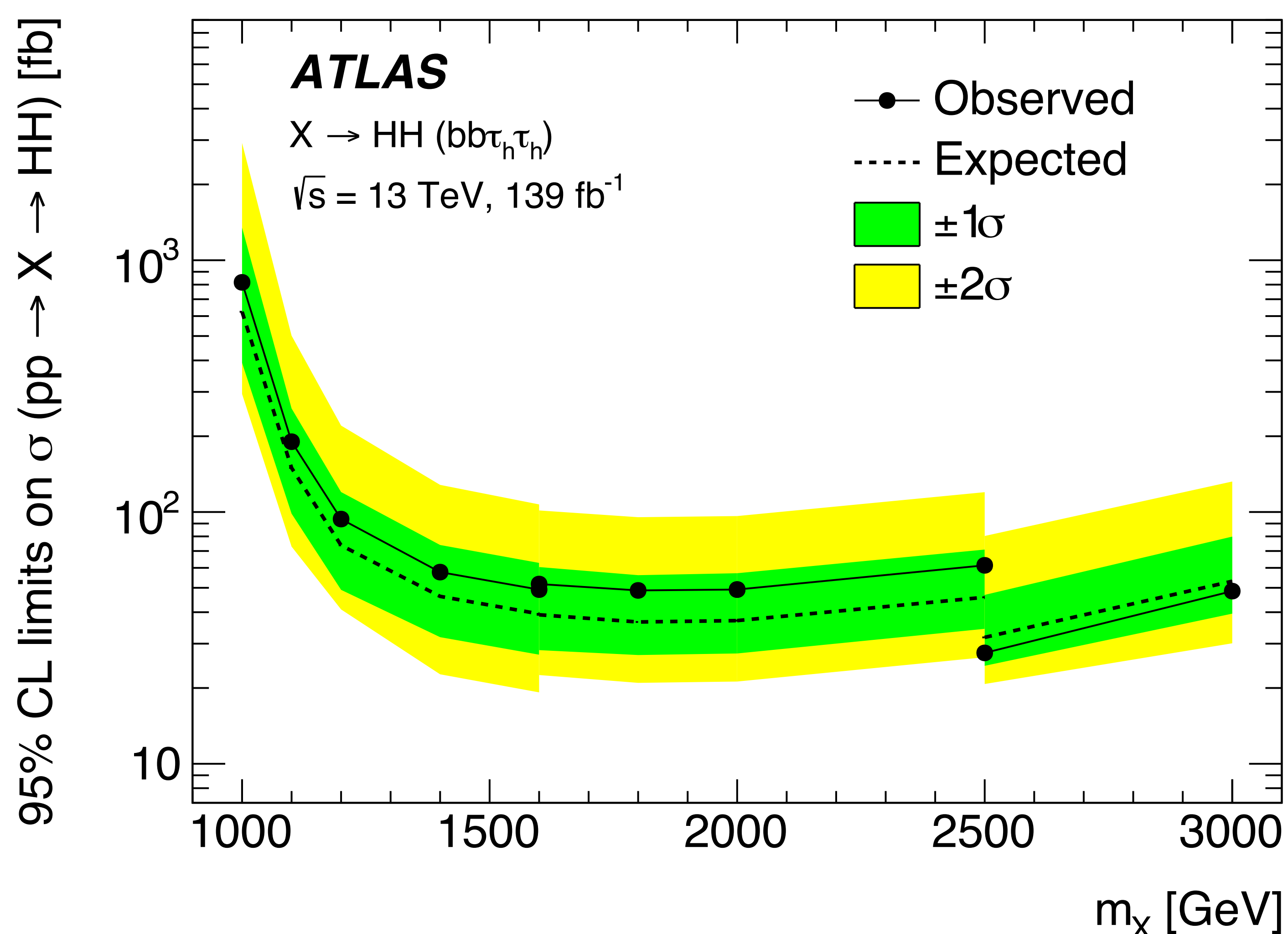

Parallel session talk by Bowen Zhang (NJU)

Prospects at High Luminosity LHC

Prospects at HL-LHC (3000fb^{-1})

Reviews in Physics 5 (2020) 100045

Significance from each analysis and their combination, w/ and w/o systematics :

	Statistical-only		Statistical + Systematic	
	ATLAS	CMS	ATLAS	CMS
$HH \to b\bar{b}b\bar{b}$	1.4	1.2	0.61	0.95
$HH \to b\bar{b}\tau^+\tau^-$	2.5	1.6	2.1	1.4
$HH \to b\bar{b}\gamma\gamma$	2.1	1.8	2.0	1.8
$HH \to b\bar{b}VV^*$	-	0.59	-	0.56
$HH \to b\bar{b}ZZ(4\ell)$	-	0.37	-	0.37
Combination	3.5	2.8	3.0	2.6
	4.5σ		4.0σ	

- Each experiment is able to reach to 3σ significance at the end of HL-LHC, in all channels combination → 4.0σ from ATLAS+CMS combination.

Prospects at HL-LHC ($3000 fb^{-1}$)

Reviews in Physics 5 (2020) 100045

Constraints on Higgs self-coupling (κ_λ)

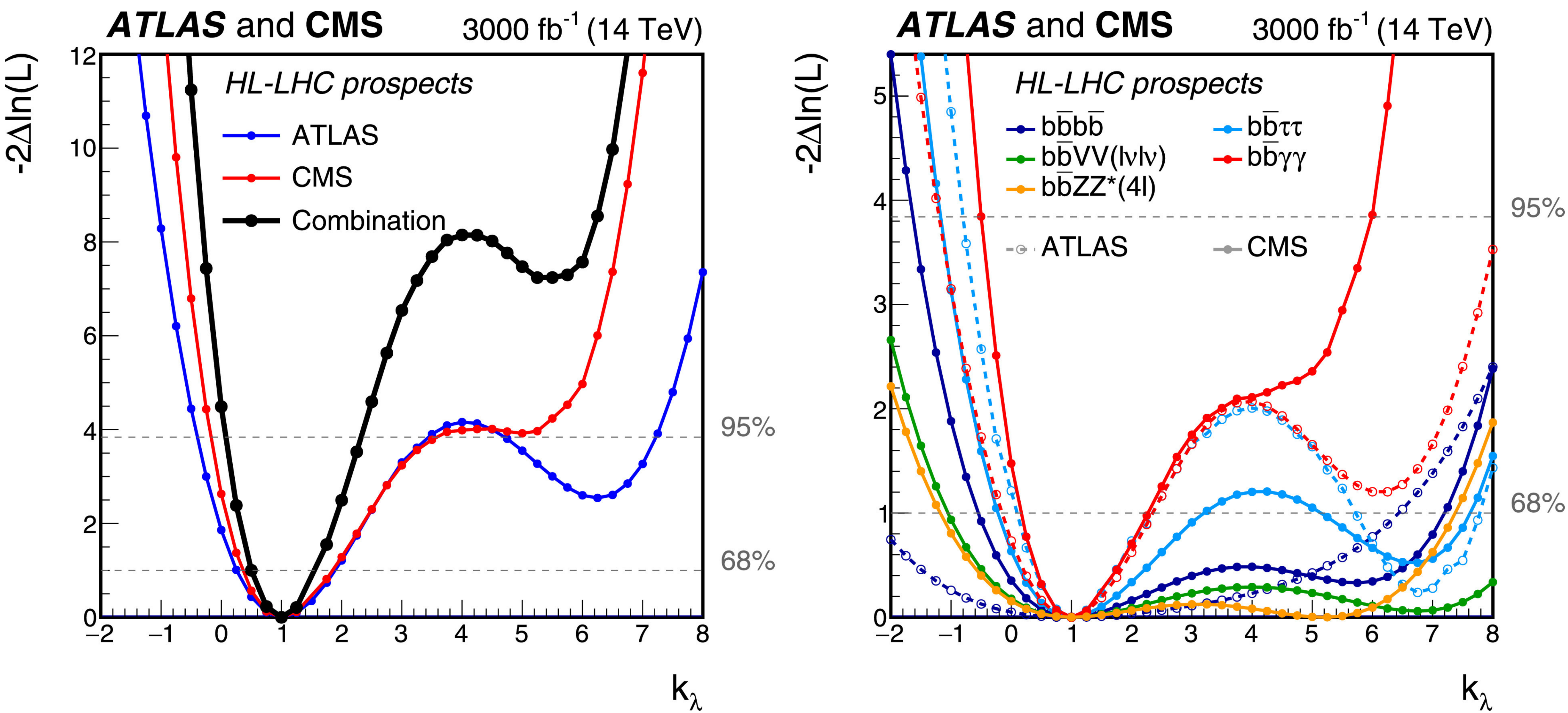

- ATLAS+CMS HH combination can set strong constraints on κ_λ parameter: [0.1, 2.3] at 95% C.L. and [0.5,1.6] at 68% C.L.

Summary

- Searching for Higgs pair productions have been performed in ATLAS and CMS
  - observed (expected) limit on σ_{HH}: 6.9 (10) and 7.7(5.2)
  - constraints on Higgs self-coupling (κ_λ): [-5.0, 12.0] and [-3.3, 8.5]
  - constraints on VVHH coupling (κ_{2V}): [-0.76, 2.90] and [-1.3, 3.5]
  - most channels with ~36fb^{-1} dataset (partial run 2 dataset)
- More results using full Run 2 dataset are in preparation !
- Perspective shows strong HH evidence at the end of of HL-LHC.

Welcome to join Di-Higgs 2020 workshop !

Nov. 19-21, 2020 @TDLI/SJTU, Shanghai

https://indico-tdli.sjtu.edu.cn/event/283/

Di-Higgs 2020: Opportunities and Challenges

19-21 November 2020
The Redding Mann Hotel/雷汀曼精选酒店(交大店)
Asia/Shanghai timezone

- Overview
- Timetable
- Contribution List
- Registration
- Participant List
- Accommodation
- Transportation

The study of di-Higgs production at the LHC and prospective future high-energy colliders provides a unique window on the dynamics of electroweak symmetry-breaking. Within the Standard Model, non-resonant di-Higgs production provides access to the Higgs tri-linear self-coupling, providing a key test of the Higgs mechanism. Beyond the Standard Model, both resonant and non-resonant di-Higgs production are sensitive to extended Higgs sectors and their implications for a possible first order electroweak phase transition in the early universe. Experimentally, di-Higgs production offers a rich array of channels to be studied, with their associated challenges.

This workshop will bring together theorists and experimentalists to discuss the theoretical implications and interpretation of di-Higgs production, the status of planned di-Higgs searches at the LHC, and the opportunities for new experimental searches at the LHC and beyond.

Self-coupling constraints in single Higgs analyses

A varied Higgs trilinear coupling effects not only inclusive Higgs production/decay rates but also their kinematics, through NLO EW corrections.

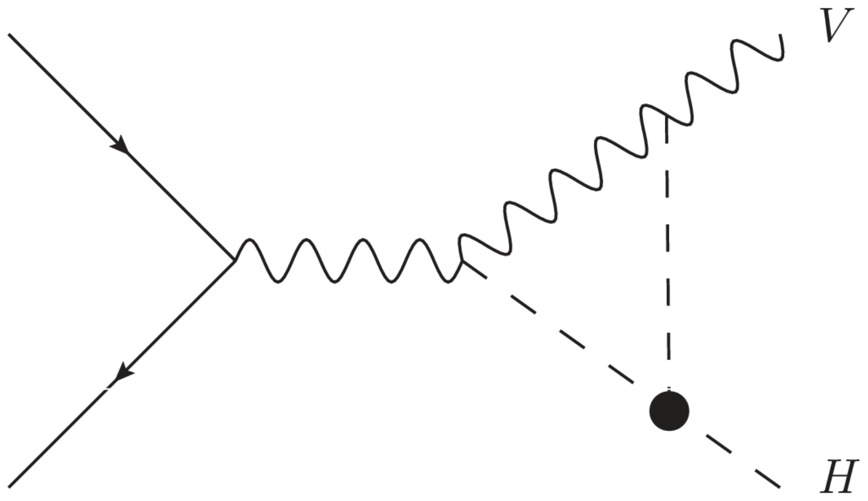

ATLAS measurement as inputs (80fb^{-1}):

- inclusive X-section for ggF, ttH
- STXS measurements for VBF and VH.

Constraints on self-coupling modifier

$$\kappa_\lambda\ (\lambda_3/\lambda_3^{SM}) \in [\text{-}3.2, 11.9]\ @\ 95\%\ \text{C.L.}$$

→ this result is comparable with direct measurement from di-Higgs channel with 36 fb^{-1} luminosity, combination:

$$-2.3 < \kappa_\lambda < 10.3 \text{ at } 95\% \text{ CL}$$

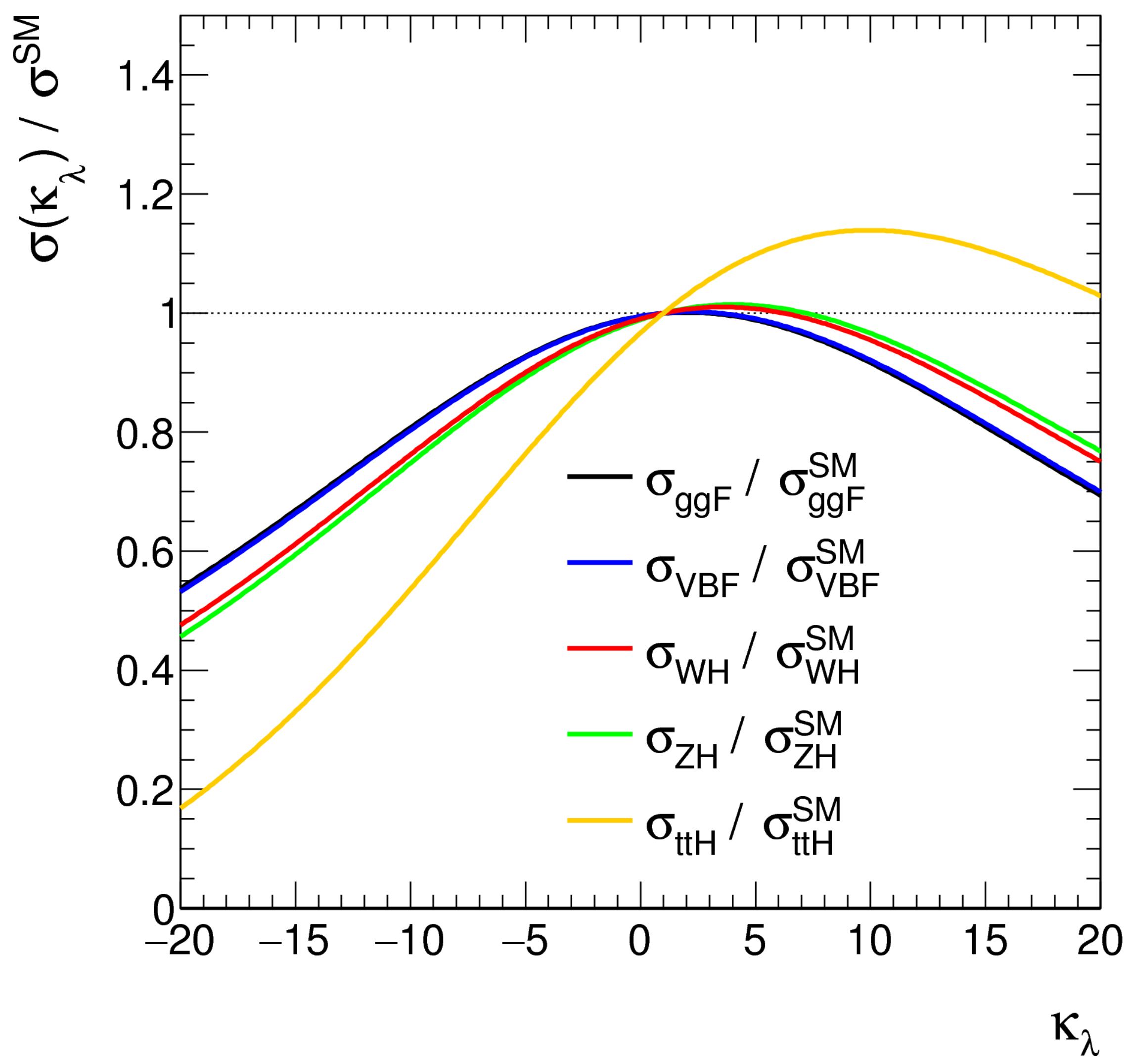

HH signal acceptance times efficiency vs κ_λ